Quaternary Research 84 (2015) 246–254

Contents lists available at ScienceDirect

Quaternary Research

journal homepage: www.elsevier.com/locate/yqres

A 15,400-year record of climate variation from a subalpine lacustrine sedimentary sequence in the western Nanling Mountains in South China

Wei Zhong [a,*], Jiayuan Cao [b], Jibin Xue [a], Jun Ouyang [a]

[a] School of Geography Sciences, South China Normal University, Guangzhou 510631, China
[b] School of Tourism, Henan Normal University, Xinxiang 453007, China

ARTICLE INFO

Article history:
Received 22 September 2014
Available online 20 June 2015

Keywords:
Lacustrine sequence
Western Nanling Mountains
Asian summer monsoon
Last deglaciation
Climate variability

ABSTRACT

Multi-proxy records of a subalpine lacustrine sequence in Daping Swamp in the western Nanling Mountains provide evidence for exploring climate variability in the past 15,400 yr. Two dry and cool (15,400–14,500 and 13,000–11,000 cal yr BP) and one humid and warm interval (14,500–13,200 cal yr BP), which we correlate to Heinrich Event 1, the Younger Dryas and the Bølling-Allerød event respectively, are revealed. The early Holocene climate (11,000–8000 cal yr BP) was characterized by less humid and warm conditions, suggesting a weaker Asian summer monsoon (ASM) intensity. Our findings indicate that the Holocene optimum occurred between 8000 and 4500 cal yr BP, and the most intensified ASM appears from 8000 to 7000 cal yr BP. After 4500 cal yr BP, climate shifted to relatively cool and dry conditions. We speculate that five short dry and cool events centered at ~11,000, 9000, 8400, 6000, and 3500 cal yr BP were linked to the Holocene ice-rafting events detected in the North Atlantic. Migration of the ITCZ, and the oceanic–atmospheric circulations, particularly SST changes in the tropical Pacific may play a pivotal role in climate variation of the study region.

Introduction

The Asian summer monsoon (ASM) system is a thermodynamic atmospheric circulation induced by seasonal heating change of the Central Asian highlands, with its extreme lapse rates and resulting central Asian low-pressure system during summer. The monsoon contributes to the atmospheric heat budget in the Northern Hemisphere and hence, changes in the monsoon system have great potential to control global climatic change (Wang et al., 1999; An, 2000). Detailed understanding of past summer monsoon climate variation, especially the precipitation-related variations during the Holocene, is also essential for predicting regional climate change in the future. The Indian summer monsoon (ISM) and East Asian summer monsoon (EASM) are two important components of the ASM system, varying on both millennial and orbital time scales. However, several important questions on specific details of monsoon climate have not been fully answered: 1) Did the two monsoon systems behave similarly or differently in East Asia, and what forcings have driven changes in the two systems (Hong et al., 2005, 2010; Shinozaki et al., 2011; Stebich et al., 2011; Zhang et al., 2011)? 2) Is there an asynchronous Holocene optimum throughout the monsoon region? 3) Has rainfall in the EASM region been increasing since the early Holocene (Zhang et al., 2011)? To fully address these questions, more paleoclimate data from typical regions influenced by both monsoon systems are needed.

The Nanling Mountains (NLM) form an important geographic division between the middle and southern subtropical zones in China, and are located at the center of the area influenced by the tropical monsoon (Gao et al., 1962). Paleoclimate studies in the eastern NLM have demonstrated that the mountains present ideal paleo-monsoon geo-archives (Zhou et al., 2004; Xiao et al., 2007; Zhong et al., 2010a, 2010b). However, there have been few relevant studies in the western NLM, which are in the transitional belt between the EASM and ISM systems (Fig. 1a) (Qian et al., 2007; Zhang et al., 2011). Because the study region is influenced by both the ISM and EASM, detailed paleoclimate studies of this area would facilitate valuable understanding of the issues mentioned above. In this study, we present a new ~15,400-yr climatic record, derived from lacustrine sediments in Daping Swamp in the western NLM. We use these data to explore the history of ASM variations since the last deglaciation in the study region.

Material and methods

Site description

Daping, a sub-alpine intermontane basin, is in the Nanshan Pasture of Chenbu Miao Autonomous County in western Hunan Province of China. This region is in the southern Bashili Grand Mountains, part of the Xuefeng Mountains in the western NLM (Fig. 1). The current annual average temperature is 10.9°C and annual precipitation about 2000 mm. Local humidity and temperature conditions lead to flora that is

* Corresponding author. Fax: +86 20 85215910.
E-mail address: DL06@scnu.edu.cn (W. Zhong).

http://dx.doi.org/10.1016/j.yqres.2015.06.002
0033-5894/

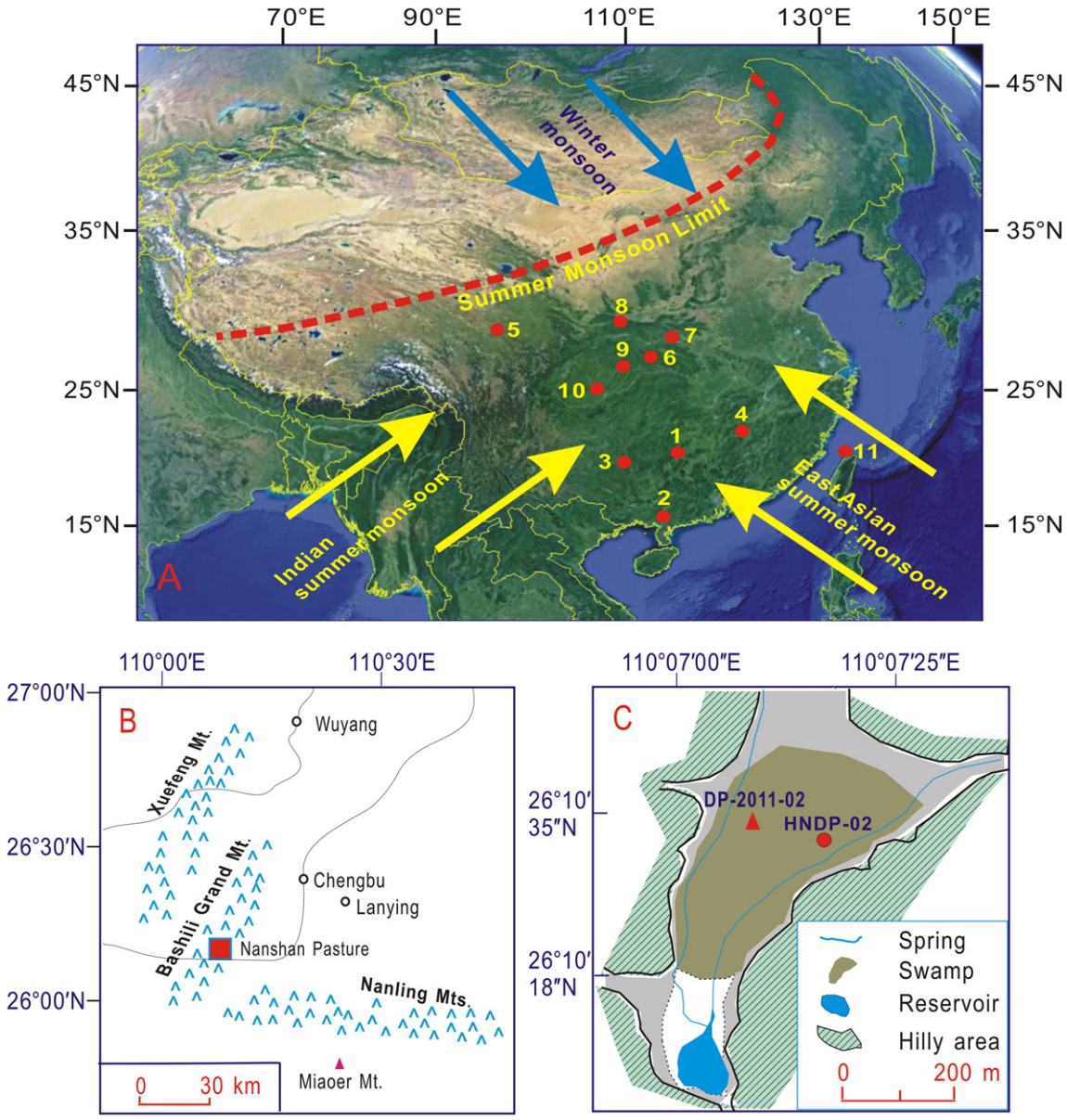

Figure 1. Climatic background of the sub-alpine Daping Swamp in the western Nanling Mountains. Dashed red line represents the averaged modern summer Asian monsoon limit. The locations of various Asian monsoon records in China referred to in the text are shown: 1, the location of Daping Swamp (B) and the core site (C) (this study); 2, Huguangyan Maar Lake in Leizhou Peninsula in South China (Yancheva et al, 2007); 3, Dongge Cave in southwest China (Wang et al, 2005); 4, Dahu Swamp in east Nanling Mountains (Zhong et al., 2010a); 5, Hongyuan peat on the eastern fringe of Tibetan Plateau (Hong et al, 2005); 6, Heshang Cave in Central China (Hu et al., 2008); 7, Sanbao Cave in central China (Wang et al., 2008a, 2008b); 8, Jiuxian Cave in central China (Cai et al., 2010); 9, Lianhua Cave in central China (Zhang et al., 2013); 10, Shigao Cave in southwest China (Jiang et al., 2012); 11, Retreat Lake in northeast Taiwan (Selvaraj et al., 2007). The red triangle indicates the location of core DP-2011-02 used in this study. The red circle indicates the HNDP-02 peat section which has been studied (Zhong et al., 2014).

dominated by evergreen and deciduous broadleaf forest, montane coppice such as *Machilus rehderi*, *Cyclobalanopsis*, *Fagus*, and *Alnus*, as well as shrub vegetation dominated by *Enkianthus* and *Rhododendron* and others (Xiao et al., 1986). Natural vegetation in the region has been substantially destroyed by modern anthropogenic activity. Present plants at the center of Daping basin are dominated by *Polygonum hydropiper*, *Juncus effuses*, *Eragrostis ferruginea*, and *Cyclobalanopsis* (*Thunb.*).

In Daping Basin, granite bedrock formed a near-surface aquiclude that trapped water and established favorable conditions for the development of Daping Swamp, which is about 300 m long and 150 m wide. This swamp has peaty sediments. Geologic investigation has revealed that buried peat accumulation there amounts to more than 100,000 m^3 (Sun and Zhang, 1984). In 1950s, a small reservoir was built in the swamp area.

Sampling and analyses

In September 2011, we recovered several cores at Daping Swamp (see also Zhong et al., 2014). A 236-cm-long core (core DP-2011-02; 26°32.02′N–110°08.03′E; ~1620 m asl) was selected for paleoclimatic investigation. In the field, the core was split lengthwise, photographed and described. Because the top 10 cm of the core had substantial modern plant roots, sample collection concentrated on 10–226 cm depths. Samples were taken at continuous 3-cm intervals for pollen measurement. Bulk dry density (DD), humification degree (HD), loss on ignition (LOI), and particle grain size fraction (PGSF) were analyzed for samples at continuous 2-cm intervals.

Eight bulk samples were measured for radiocarbon dating at the Key Laboratory of Western China's Environmental Systems (Ministry of

https://doi.org/10.1016/j.yqres.2015.06.002 Published online by Cambridge University Press

Education of China) at Lanzhou University. Radiocarbon ages were calibrated using the Calib 6.0 program with respect to IntCal09 (Reimer et al., 2009) (Table 1, Fig. 2). The chronological sequence for the core was established based on the mean sedimentation rate between two adjacent calibrated ages, using linear interpolation for samples.

For pollen measurement, before being subjected to a heavy-liquid separation procedure using sodium polytungstate to assist heavy mineral removal, the samples were treated with 10% HCl, 10% KOH, and sieved using 7-μm nylon mesh (Fægri and Iversen, 1989a, 1989b; Bolch, 1997; Zabenskie et al., 2006). Following this stage, the samples were treated with a hydrofluoric acid and acetolysis solution, and then stored in silicone oil. One tablet of *Lycopodium* marker spores was added to each sample for estimating pollen concentration.

LOI, a proxy commonly used to estimate sediment total organic matter (TOM) (Bengtsson and Enell, 1986; Heiri et al., 2001), was determined by burning the samples for about 2.5 h at 550°C, after they had been grounded and homogenized. After being treated with 0.1 mol/L NaOH and boiled for 1 h to extract humic acid, the solution was filtered and diluted. We used a UV-1901 spectrophotometer to measure absorbance of the solution at wavelength 520 nm. Analytical accuracy was 1%. We expressed the absorbance relative to that of distilled water (defined as 0%), and used it to express HD. In this study, we use calibrated HD (HD_{cal}) to indicate the intensity of humification (Zhong et al., 2010a, 2010b): $HD_{cal} = HD/(M_{sample} \times TOM)$, where HD_{cal} is the corrected absorbance value, HD is the raw absorbance value, M_{sample} is weight of the sample for measurement, and TOM is the percentage of TOM represented by values of LOI (Zhong et al., 2010b). Higher or lower HD_{cal} values represent stronger or weaker humification intensity, respectively.

DD was measured as weight of the dry mass per unit volume (Janssens, 1983). Dry mass of exactly defined 1 cm^3 volume was determined by oven drying at 50°C until a constant weight was achieved. To analyze PGSF, we pretreated the sample with 10–20 ml of 30% H_2O_2 to remove organic matter, and then with 10 ml of 10% HCl to remove carbonates. We added approximately 2 L of deionized water. After 24 h, sample residue was treated with 10 ml of 0.05 M $(NaPO_3)_6$ on an ultrasonic vibrator for 10 min. The Malvern Mastersizer 2000 particle-size analyzer automatically yields percentages of related grain size fractions of a sample, with relative error less than 1%.

Results

Radiocarbon dating results of core DP-2011-02 are listed in Table 1 (also in Fig. 2). The bottom age was determined to be 15,400 cal yr BP. The surface soil (Unit DP-1, 0–10 cm) of the core contains a large number of modern plant roots of *Polygonum hydropiper* and *Juncus effuses*. Unit DP-2 (10–80 cm) is primarily composed of dark-gray herbaceous peat. This unit is underlain by DP-3 (80–137 cm), which is characterized by dark-gray sand and silt containing fine sand and minor amounts of small gravel (<0.3 cm). A layer of dark-gray peat appears between 137 and 143 cm depth (Unit DP-4). Unit DP-5 (143–170 cm) consists mainly of dark-gray sand and silt containing minor amounts of small gravel (<0.5 cm). Unit DP-6 (170–180 cm) is a layer of gray-brown peat bearing *Juncus effuses* remains. Below this unit, sediments are composed of gray-white sand and silt bearing minor fragments of *Rhododendron simsii Planch*. (Unit DP-7, 180–224 cm). From 224 to 236 cm, sediments consist of dark-gray peat with fragments of *Polygonum hydropiper* and *Juncus effuses* (Unit DP-8). Below this unit, materials are of gray-yellow coarse sand and fine gravel (≤2 cm) (DP-9) (Fig. **2**).

In the core, the average pollen density is 140,603 grains/g sample, and the average number of counted pollen and spores is 525 grains/sample. About 150 pollen and spore types were identified. The pollen assemblage is dominated by tree plants with average percentage 58.5%, and mean percentages of herb-pollen and fern spores are 33.6% and 7.9%, respectively. Tree-pollen species consist mainly of *Cyclobalanopsis*, *Fagus*, *Betula*, *Pinus*, and *Carpinus*, with small amounts of *Castanopsis*/*Lithorcarpus*, *Altingia*/*Liquidambar*, *Alnus*, *Zelkova*, *Quercus*, *Corylus*, and Moraceae. Herb-pollen consists mainly of Poaceae, Cyperaceae, *Ranunculus*, and small amounts of *Artemisia*, *Lagopsis*, and Scrophulariaceae. Fern spores consist mainly of *Microlepria*, Polypodiaceae, *Athyrium*, and monolete spores. In the study, we use total tree-pollen and total herb-pollen, as well as the abundance of specific pollen taxa to infer past climatic conditions (Fig. 3).

The HD_{cal} values of samples of core DP-2011-02 vary between 3.2 and 17.3 with a mean of 9.3. The DD values are from 0.11 to 0.79 g cm^{-3} with an average of 0.39 g · cm^{-3}, and TOM varies from 6.4% to 50.7%, and averages 18.6% (Fig. 4). PGSF analysis indicates the sand fraction varies from 23.3% to 77.3% with a mean of 52.5%. The silt fraction varies between 19.3% and 68.0%, and averages 42.6%. The clay fraction is from 2.3% to 10.3% with a mean of 4.9%.

Discussion

Climatic implication of multi-proxy records

Variation of lithology

In core DP-2011-02, the litho-unit DP-9 may have originated from underlying granite weathering crust (Fig. 2). Input of materials to Daping Swamp is mainly derived from the surrounding hilly area and transported by the surface runoff. Shifts in organic-rich (i.e., peat or organic mud, for example, DP-2, DP-4, DP-6 and DP-8) and organic-poor (i.e., silt or fine sand, DP-3, DP-5 and DP-7) lithologic units in the core imply hydrologic variations caused by varying climatic conditions. Similar to the interpretation of the Dahu record in the eastern Nanling Mts. (Zhong et al., 2010a, 2010b), high TOM in the marshy sediments of core DP-2011-02 is considered to reflect the environmental conditions that govern peat formation. Shrinkage of the water body of the swamp in response to dry conditions would lead to terrestrial and

Table 1
Radiocarbon dating results of core DP-2011-02 in Daping Swamp in the western Nanling Mountains.

Lab. code	Field code	Depth /cm	Material	Age (^{14}C yr BP)	Calibrated age	
					cal yr BP (2 sigma)	Intercept (cal yr BP)
LUG11-198	DP-002	24–29	TOC	673 ± 87	518–743	630
LUG11-199	DP-004	54–59	TOC	2218 ± 113	1924–2491	2210
LUG11-200	DP-005	67–72	TOC	3768 ± 94	3901–4415	4160
LUG11-201	DP-006	81–86	TOC	4119 ± 95	4420–4848	4630
LUG11-202	DP-008	108–113	TOC	5428 ± 158	5892–6565	6230
LUG11-204B1	DP-0011	151–156	TOC	8895 ± 128	9596–10243	9920
LUG11-205	DP-0012	183–188	TOC	11373 ± 127	12928–13484	13210
LUG11-206	DP-0013	223–228	TOC	12452 ± 167	13999–15149	14570

Radiocarbon dating was measured at the Key Laboratory of Western China's Environmental Systems (Ministry of Education of China) at Lanzhou University. The ages were calibrated using the Calib 6.0 program with respect to IntCal09 (Reimer et al., 2009).

https://doi.org/10.1016/j.yqres.2015.06.002 Published online by Cambridge University Press

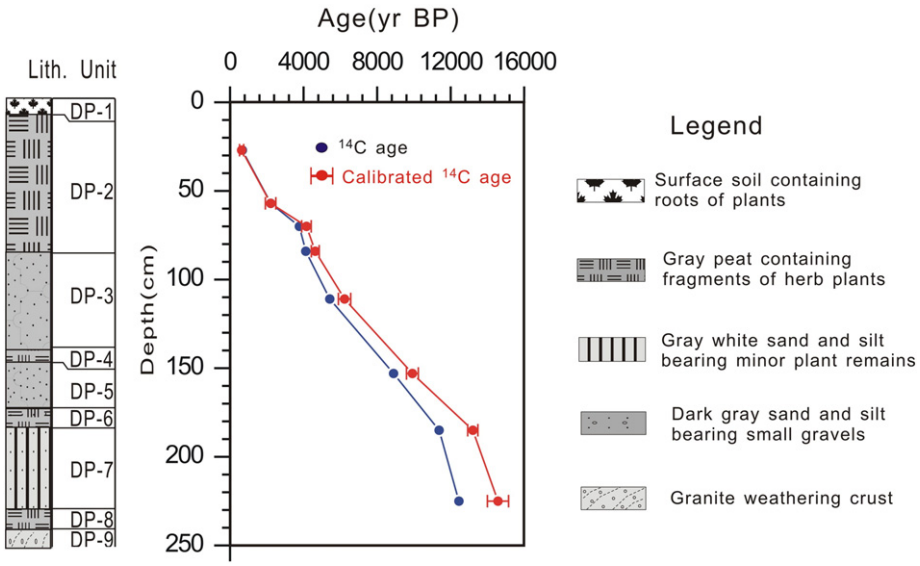

Figure 2. Stratigraphy and relationship between age and depth of core DP-2011-02 in Daping Swamp.

near-shore aquatic plants invasion, resulting in higher TOM at the core site, whereas wet conditions would result in water body expansion, thus favoring deposition of organic-poor sediments.

Pollen, HD, TOC, DD and PGSF

In the study region, it is generally accepted that variations in total tree-pollen and herb-pollen are closely related to climatic variations: wet and warm conditions result in high total tree pollen, whereas dry and cool conditions favor overgrowth of herbs, thus leading to high total herb pollen. Previous studies have demonstrated that *Fagus* and *Castanopsis/Lithocarpus* are sensitive to winter temperatures with high percentages of *Fagus* and *Castanopsis/Lithocarpus* representing warm/wet and low percentages dry/cool conditions, respectively (Liu and Hong, 1998; Zhou et al., 2004; Xiao et al., 2007).

HD is a proxy to describe the intensity of decomposition of plant remains. Because the process of decomposition of dead plants is closely associated with local climate conditions, this proxy can be used to reflect changes of sedimentary environment or paleoclimate. A number of studies have demonstrated that the HD of peat is a sensitive indicator of past climate changes (Aaby, 1976; Chamber et al., 1997; Christopher and John, 2000; Charman et al., 2001; Wang et al., 2010; Zhong et al., 2010b). Based on experimental studies, Chai (1993) revealed that there exists a nonlinear influence between soil moisture and temperature and the decomposition rate of plants; microbial decomposition of plant remains is very weak with soil temperature below 5°C and soil humidity less than 20%. However, with increases in soil temperature and humidity, microbial activity increases rapidly. This activity peaks at soil temperatures about 30°C and soil humidity around 60–80%. Therefore, more humid conditions, which generally suggest warmer conditions in Asian summer monsoon-influenced regions of China (Yao et al., 1996), would promote vegetation production and provide more plant remains for decomposition. In turn, this would increase humic acids in peat. In contrast, dry and cool conditions reduce vegetation production (i.e., lower TOM) and weaken microbial decomposition, which would decrease humic acids in the peat. In this study, we used HD_{cal} to reflect humification intensity, with higher HD_{cal} implying relatively wetter and warmer conditions, and vice versa.

The DD and PGSF can provide information on external input of clastic materials to the lake. Generally, relatively wet and warm conditions would elevate riverine/fluvial inputs to the swamp, favoring higher input of clastic materials that produce high DD and relatively coarser materials (e.g., higher sand fraction), whereas relatively dry and cool conditions would cause low DD and high silt and clay fraction values.

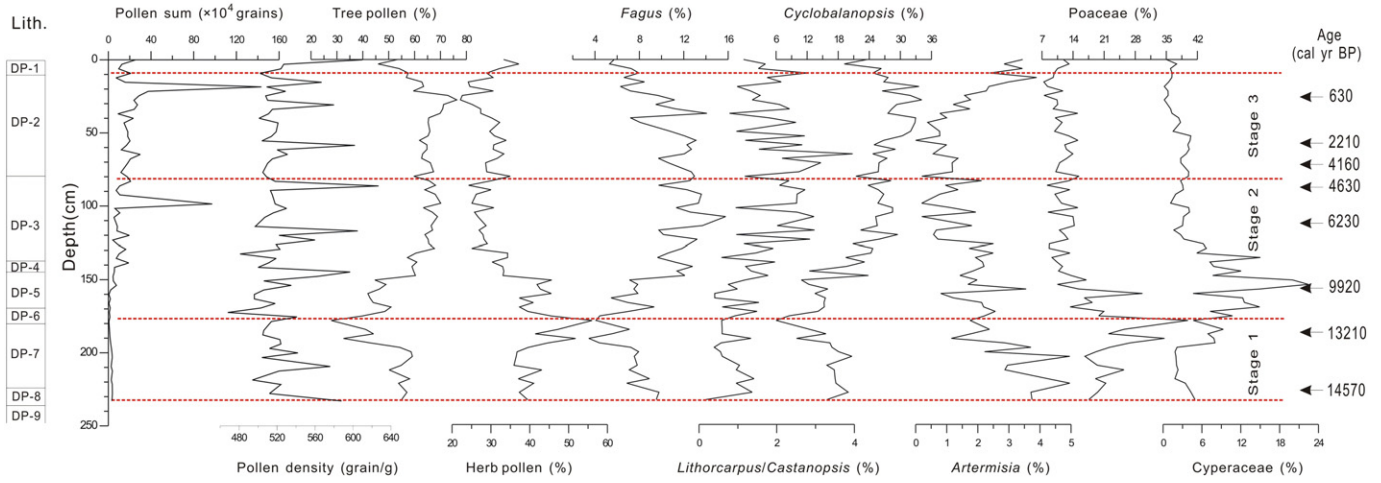

Figure 3. Pollen results for core DP-2011-02 in Daping Swamp are shown together with depth, litho-units, and ^{14}C calibrated ages. The red dashed lines indicated the climatic stages reflected by multi-proxy records.

https://doi.org/10.1016/j.yqres.2015.06.002 Published online by Cambridge University Press

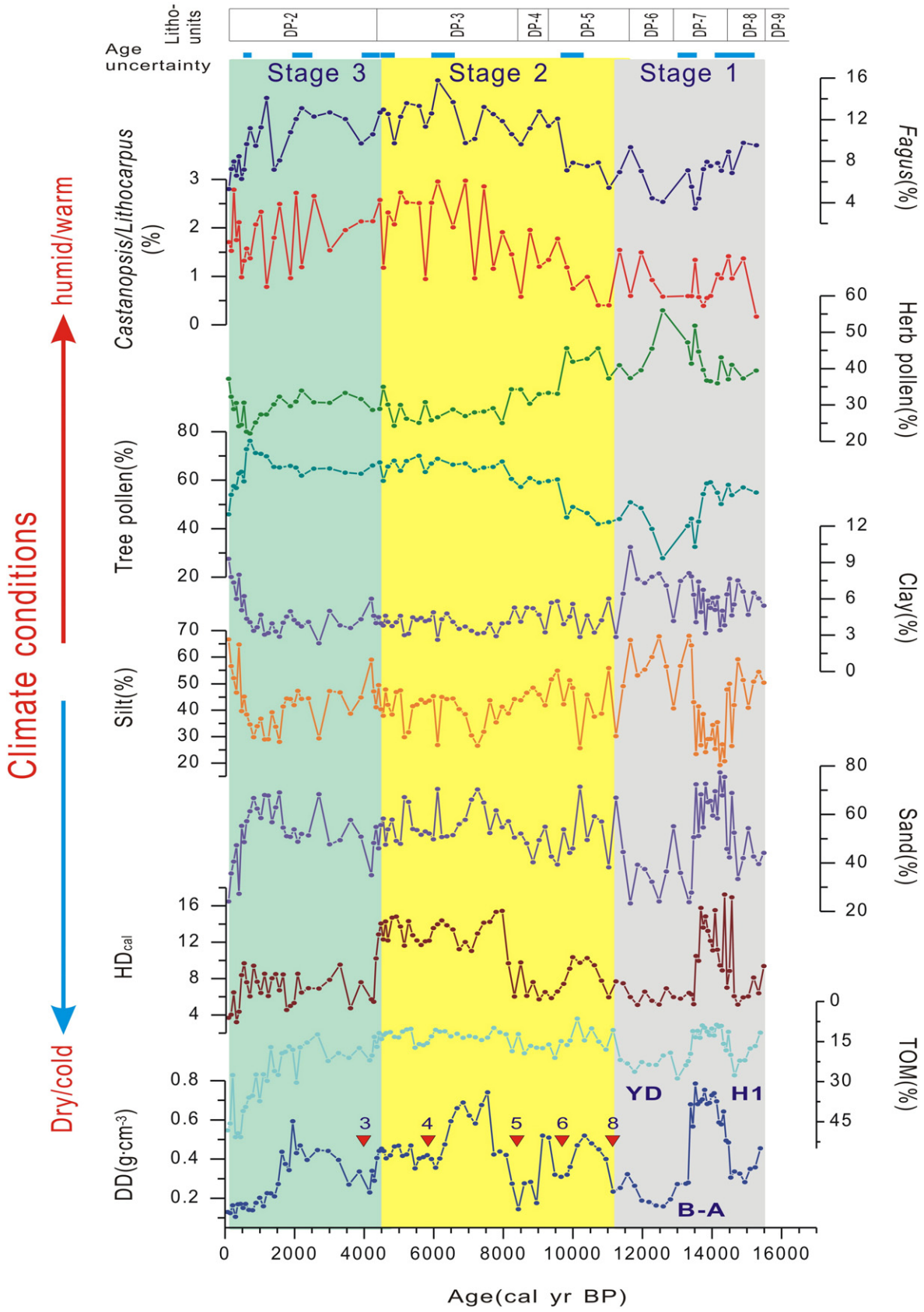

Figure 4. Litho-units and multi-proxy records including pollen records, bulk dry density, total organic matter, calibrated humification degree, and grain-size fractions of core DP-2011-02 core in Daping Swamp. Eight bulk ^{14}C dates are shown with an uncertainty interval of 2σ. The cold Heinrich Event 1 (H1), the Bølling and Allerød (B-A) warming event, and the Younger Dryas cold event (YD) are reflected. The red triangles indicate the millennial dry and cool oscillations that possibly correspond to the North Atlantic ice-rafting events (i.e., Bond Events 3, 4, 5, 6, and 8) (Bond et al., 2001). The gray, green and yellow bars represent the climatic stages reflected by multi-proxy records.

https://doi.org/10.1016/j.yqres.2015.06.002 Published online by Cambridge University Press

Climatic variability over the past 15,400 yr

Because the climate of the study region was strongly influenced by ASM (including EASM and ISM), climatic conditions reflected by multi-proxy records from Daping Swamp were closely related to the varying strength of ASM: a strengthened ASM generally results in higher precipitation and temperatures, whereas a weakened ASM favors relatively dry and cold conditions (Herzschuh, 2006). Based on the proxy records, three climatic stages can be identified over the past 15,400 yr.

Stage 1 (15,400–11,000 cal yr BP; 236–170 cm depth)

The pollen sum was very low. Percentages of *Cyclobalanopsis* and *Fagus* were relatively low, but those of Poaceae and *Artemisia* were generally higher (Fig. 3), indicating overall **a** dry and cool environment. This period can be divided into three sub-periods. From 15,400 to 14,500 cal yr BP, sharp declines in DD, HD_{cal}, and sand fraction, as well as an increase in TOM (Fig. 4) corresponding to a peat layer (Unit DP-8; Fig. 2), suggest distinctly dry conditions that were likely related to weakening of the ASM. It should be mentioned that due to relatively low sampling resolution, our pollen data may not reflect this short dry period. This interval may *sensu lato* coincide with Heinrich event 1 (H1) that was detected in the North Atlantic (Heinrich, 1988; Stanford et al., 2011). In contrast, from 14,500 to 13,200 cal yr BP, high tree pollen and low herb pollen concentrations and significant increases in DD, HD_{cal}, and sand fraction, and a clear reduction in TOM all reflect a wet and warm climate that may have resulted from an intensified ASM. This short period could correspond to the Bølling-Allerød. These two millennial-scale events were also reflected by stalagmite $\delta^{18}O$ records in East and Central China (Wang et al., 2001; Dykoski et al., 2005; Wang et al., 2008a, 2008b; Zhou et al., 2009; Fig. 5), and lake sediments in both tropical South China (Yancheva et al., 2007) and the northeastern Qinghai–Tibet Plateau (Ji et al., 2005).

In contrast to the significantly wet and cool conditions during the Younger Dryas (YD) chronozone reflected in Dahu Swamp in eastern NLM (Zhou et al., 2004), our results show sharp declines of total tree-pollen, *Cyclobalanopsis* and *Fagus*, and increases of total herb-pollen, Poaceae, and Cyperaceae in the period of 13,000–11,000 cal yr BP (Figs. 3 and 4), suggesting dry and cool conditions caused by a weakened ASM intensity. This interpretation is supported by synchronous declines in DD, HD_{cal}, and sand fraction, an increase in TOM (Fig. 4) and the development of a peat layer at this interval in the stratigraphy (Unit DP-6, Fig. 2). This interval, which can be correlated with the Younger Dryas chronozone, has been also widely detected from various Asian monsoon records in China, for example, from Dahu Swamp in the eastern NLM (Zhou et al., 2004; Zhong et al., 2010a), Huguangyan maar lake in Leizhou Peninsula (Yancheva et al., 2007), the South China Sea (Wang et al., 1999; Kienast et al., 2001), stalagmite records in East and Central China (Wang et al., 2001; Wang et al., 2008a, 2008b; Zhang et al., 2013), and Southwest China (Dykoski et al., 2005).

Stage 2 (11,000–4500 cal yr BP; 170–80 cm depths)

During this stage, total tree-pollen concentration, as well as percentages of *Cyclobalanopsis*, *Castanopsis*/*Lithocarpus*, and *Fagus* were relatively high, whereas total herb pollen, Poaceae, and Cyperaceae percentages are relatively low (Fig. 3). It can be observed that total tree-pollen concentration increased after ~9000 cal yr BP and remained around 70% until present, suggesting relatively stable ecological/environmental conditions. Varying values of TOM, DD, HD_{cal}, as well as sand and silt fractions (Fig. 4) possibly reflect hydrologic variations. From 11,000 to 4500 cal yr BP, these proxy records indicate general wet and warm conditions associated with an enhanced ASM intensity. Similar results were also inferred for the stalagmite $\delta^{18}O$ record from Jiuxian Cave (11,800–4500 yr) (Cai et al., 2010) and Lianhu Cave (10,600–4200 yr) (Zhang et al., 2013) in Central China. However, the Daping record does not suggest that the early Holocene (11,000-8000 cal yr BP) was the warmest and most humid interval. A similar situation was also found in the stalagmite $\delta^{18}O$ record of Heshang Cave in the middle reach of the Yangtze River (Fig. 5h; Hu et al., 2008), Lianhua Cave in Central China (Fig. 5i; Zhang et al., 2013), and the TOC record of Retreat Lake (Fig. 5k; Selvaraj et al., 2007). This interpretation is contradicted by peat- (Fig. 5f and c; Hong et al., 2005; Zhong et al., 2010a), stalagmite- (Fig. 5e; Dykoski et al., 2005), lacustrine sediment- (Fig. 5g; Yancheva et al., 2007), and pollen-based (Liew et al., 2006; Wang et al., 2007) Asian monsoon reconstructions in China.

High DD values reveal a warm and humid period from 8000 to 6000 cal yr BP (Figs. 4 and 5). From 8000 to 4500 cal yr BP, low TOM and high values of HD_{cal}, DD, and sand and silt fractions, reflect evidently wet and warm conditions. High total tree pollen, *Cyclobalanopsis*, *Castanopsis*/*Lithocarpus*, and *Fagus* percentages, in combination with low total herb pollen, Poaceae, and Cyperaceae (Figs. 3 and 4) reveal a distinct wet and warm environment that may relate to an intensified ASM. The most significantly wet period from 8000 to 6000 cal yr BP could be considered as the "Holocene Optimum". This period is very close to the maximum average growth rate exhibited between ~8000 and 5500 yr BP in stalagmite D4 from Dongge Cave (Dykoski et al., 2005), and the timing of its onset is very similar with the conventional Holocene Optimum between ~8500 and 3000 yr (Shi et al., 1993), but the termination occurs much earlier.

Stage 3 (4500–0 cal yr BP; 80–10 cm depths)

Although the total tree pollen declined slightly at ~4500 cal yr BP, the *Castanopsis*/*Lithocarpus* and *Fagus* percentages displayed an obvious decreasing trend while the total herb pollen, Poaceae, and Cyperaceae percentages increased (Figs. 3 and 4), suggesting a shift towards dry and cool conditions. This interpretation is supported by the lithology of the unit, which is characterized by dark-gray herbaceous peat, and the sharp decrease in HD_{cal} and increase in TOM (Figs. 2 and 4). A decrease in moisture around 4400–4000 cal yr BP was widely recorded by lower lake levels in China, India and Africa, as well as by widespread cultural collapse in low-latitude regions (Wang et al., 2005). From 4000 to 3500 cal yr BP, synchronous decreases in DD, HD_{cal}, and sand fraction, as well as a slight increase in TOM, indicate a short dry and cool period that might coincide with Bond event 3 (Fig. 4). However, during the interval between 2500 and 1300 cal yr BP, higher values of total tree pollen and *Fagus*, as well as relatively low total herb pollen, Poaceae, and Cyperaceae imply a short wet and warm period. After this period, multi-proxy records reflect a climate shift to dry conditions.

Possible forcing mechanisms of the climatic variations

The Daping records do not show significantly humid conditions during the early Holocene (i.e., 11,000–8000 cal yr BP) (Figs. 4 and 5b,c). One possible explanation is that glacial boundary forcing had a more dominant role in modulating the monsoon than did insolation during the early Holocene (Overpeck et al., 1996; Fleitmann et al., 2003; Ivanochko et al., 2005). The warm and humid period from 8000 to 6000 cal yr BP exhibits a ~4000 yr time lag when compared with the summer insolation anomaly at 25°N from 12,000 to 11,000 yr (Fig. 5a) (Berger and Loutre, 1991). This delayed response of monsoon intensity to insolation forcing was also observed in EASM records from subalpine Retreat Lake in northeast Taiwan (Selvaraj et al., 2007), and in the ISM records presented by Overpeck et al., (1996); Fleitmann et al. (2003, 2007). Multi-proxy records of Daping Swamp show consistency with insolation trends from 8000 yr onward (Fig. 5), indicating that long-term changes in ASM intensity likely depend on summer insolation. Additionally, the gradual long-term decrease in ASM intensity resembles various monsoon records obtained in China (Hong et al., 2003; Wang et al., 2005; Yancheva et al., 2007; Hu et al., 2008), Oman (Fleitmann et al., 2003), the Arabian Sea (Gupta et al., 2005), and Cariaco Basin off the Venezuelan coast (Haug et al., 2001) (Fig. 5). This implies the influence of the migration of the mean position of ITCZ is

https://doi.org/10.1016/j.yqres.2015.06.002 Published online by Cambridge University Press

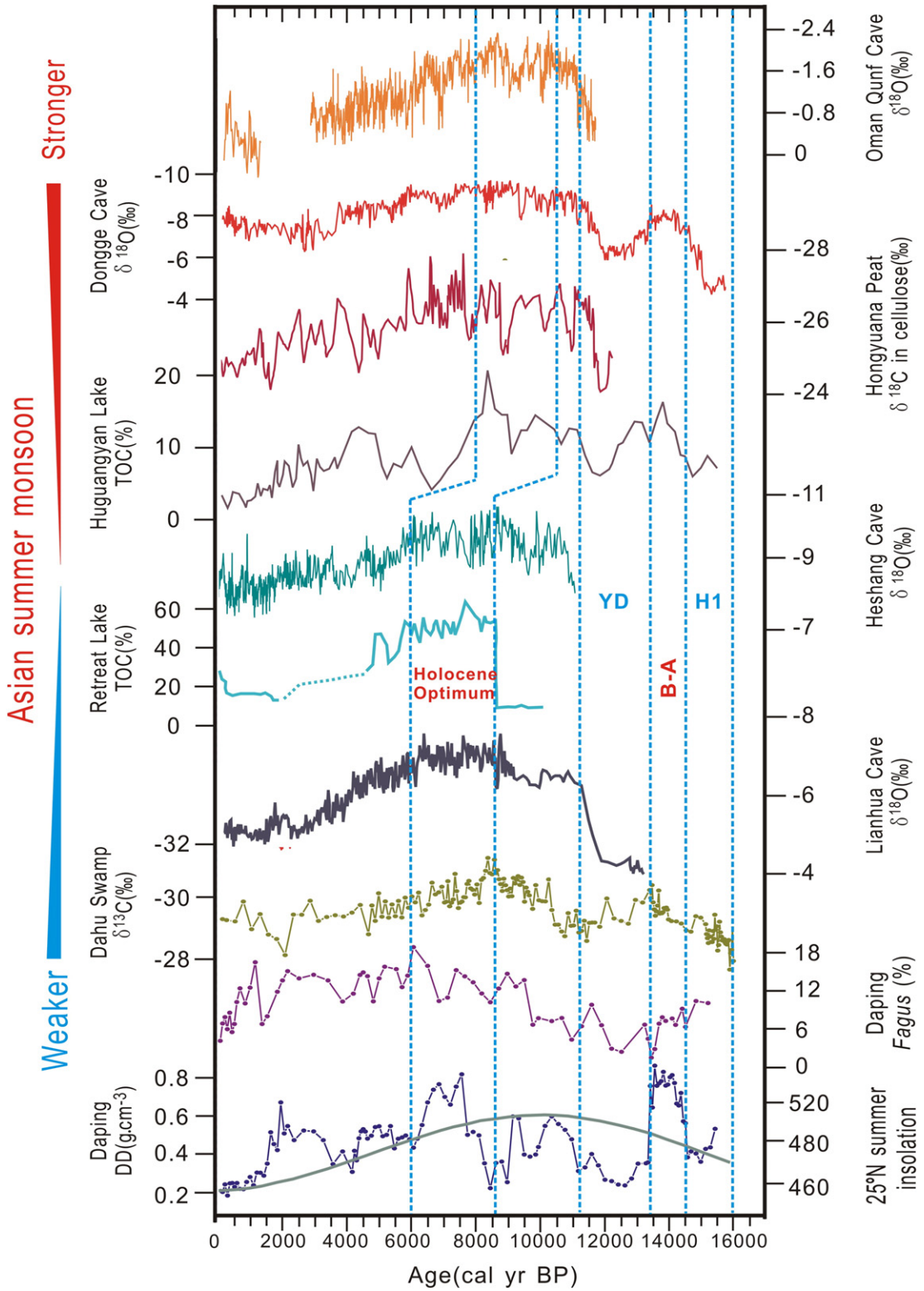

Figure 5. Correlation of Daping records with: (A) the summer insolation at 25°N (Berger and Loutre, 1991); (B) and (C) DD and *Fagus* percentage of Dahu Swamp (this study); (D) bulk $\delta^{13}C$ of Dahu Swamp (Zhong et al., 2010a); (E) stalagmite $\delta^{18}O$ of Lianhua Cave (Zhang et al., 2013); (F) TOC of Retreat Lake (Selvaraj et al., 2007); (G) stalagmite $\delta^{18}O$ of Heshang Cave (Hu et al., 2008); (H) bulk Ti of Huguangyan Maar Lake (Yancheva et al, 2007); (I) $\delta^{13}C$ in cellulose of Hongyuan peat (Hong et al, 2005); (J) stalagmite $\delta^{18}O$ of Dongge Cave (Dykoski et al, 2005); (K) stalagmite $\delta^{18}O$ records of Oman Qunf cave (Fleitman et al., 2003). The blue dashed lines indicate climatic periods that correspond to Heinrich event 1 (H1), the Bølling-Allerød (B-A), the Younger Dryas (YD) events, and the Holocene Optimum.

closely related to that of insolation. In addition, in the early- and mid-Holocene (8000–4500 yr), the tropical Pacific SST reached its Holocene average around 8500 yr in the West Pacific Warm Pool, where the EASM prevails (Gagan et al., 2004). Ocean–atmospheric interactions, particularly SST changes, in the tropical Pacific have a strong influence on the export of heat and water vapor to high latitudes and are therefore believed to be an active force in global climate change (Lea et al., 2000; Selvaraj et al., 2007). Wang et al. (1999); Jian et al. (2000) demonstrated

https://doi.org/10.1016/j.yqres.2015.06.002 Published online by Cambridge University Press

enhanced meridional heat and moisture transport from the western tropical Pacific to the North Pacific, when the EASM reached its northernmost limit and the Loess Plateau in China was greener than today (Selvaraj et al., 2007). The SSTs were mostly higher than 29°C before 5000 yr, which is consistent with the strong ASM during the Holocene Optimum revealed by the Daping records (Figs. 4 and 5). Conversely, reduced heat transport is unambiguous in the SST record with temperatures less than 29°C and a clear decrease between 5000 and 2000 yr, corresponding to a weakening of ASM. This is consistent with the evidenced of low total tree pollen, *Castanopsis*/*Lithocarpus*, *Fagus*, and HD_{cal}, and high total herb pollen and TOM in Daping Swamp (Figs. 4 and 5).

Superimposed on these long-term variations, we can identify several millennial or multi-centennial scales dry and cool phases centered at ~11,000, 9000, 8400, 6000 and 3500 cal yr BP. Acknowledging age uncertainty, these events might have coincided with Holocene ice-rafting events 8, 6, 5, 4, and 3, respectively (Fig. 4). The 9000 and 8400 cal yr BP phases could correlate with, respectively, the two cooling events that occurred at 9200 and 8200 (8000–8400) yr ago detected in the North Atlantic which have been considered to be triggered by a meltwater pulse into the North Atlantic and a resultant reduction of the thermohaline circulation (Fleitmann et al., 2008). Another climatic shift reflected at ~3500 cal yr BP is very close to the drastic dry event occurred at ~4000 yr due to weakened ASM recorded in the Dongge cave (Wang et al., 2005) and other localities in China Wu and Liu (2005).

In Daping Swamp, the termination age of the so-called Holocene Optimum is at ~6000 cal yr BP (Fig. 5). The asynchronous termination of the Holocene Optimum of various Asian monsoon records has been discussed by Jiang et al. (2012). They concluded the Holocene Optimum reflected by stalagmite $\delta^{18}O$ records ended at 7200–7400 yr in Oman within the ISM region (Fleitmann et al., 2003), at 5600–5800 yr in Central China (Hu et al., 2008; Dong et al., 2010) in the EASM region, and at ~6000–7000 yr in South China (Zhou et al., 2004; Dykoski et al., 2005; Jiang et al., 2012) where climate was influenced by both the ISM and EASM. This phenomenon may be attributed to Holocene SST dynamics in the western tropical Pacific and the principal EASM moisture source (Jiang et al., 2012). Modern meteorological data (Liu et al., 2008) indicate a precipitation anti-phasing between the ISM and EASM on annual-to-decadal time scales. With a concurrent decrease the ISM, the EASM is intensified, with northward movement of the Meiyu band, which results in abundant rainfall in central and northern China. Also, high SSTs in the western tropical Pacific could result in the enhancement of upper-level convection from the Philippines to the Sino-India Peninsula via the South China Sea, forcing the subtropical high over East Asia to move northward along with the monsoon front and rain band. This would have brought more precipitation to central and northern China (Huang et al., 2004). Climate-model simulations also suggest that an increase in the western tropical Pacific SST could have increased summer rainfall in central and northern China (Liu et al., 2003). Marine sediment geochemical proxy records inferred warm conditions in the western tropical Pacific in the early-middle Holocene, followed by a decreasing trend since ~5000 yr (Stott et al., 2004). When the ISM began to decrease and the insolation-driven ITCZ migrated southward after 7300 yr ago, the prevailing EASM, strengthened by the warm western tropical Pacific, would have enhanced landward advection of moisture and heat to the west NLM (this study) and to the middle Yangtze River and the Shennongjia districts (Hu et al., 2008; Dong et al., 2010) in subtropical China at least since ~6000 yr ago.

Conclusions

The Daping record presents a climate history since the last deglaciation. Our study reveals two distinct millennial-scale dry and cool oscillations at 15,400–14,500 cal yr BP and 13,000–11,000 cal yr BP, which may correlate with the H1 and YD cooling events. An obviously humid and warm interval between 14,500 and 13,200 cal yr BP coincides with the Bølling-Allerød warm period. In the early Holocene (11,000–8000 cal yr BP), cool and relatively dry conditions suggest a relatively weak ASM intensity possibly resulting from the continuing influence of glacial-age boundary conditions. Beginning at 8000 cal yr BP, the long-term climatic variation was similar to various Asian monsoon records obtained in South and East Asia. A distinct wet and warm period was revealed between 8000 and 4500 cal yr BP, followed by gradual weakening of the ASM. The most evident wet and warm period associated with a significantly intensified ASM appeared between 8000 and 6000 cal yr BP. The general trend of climate variability was punctuated by five short, weak ASM events centered at ~11,000, 9000, 8400, 6000, and 3500 cal yr BP. These events can be tentatively linked to Holocene ice-rafting events in the North Atlantic. This reflects that the oceanic-atmospheric circulation and shifts of the mean ITCZ position are directly affected by summer insolation and indirectly through ITCZ effects on western tropical Pacific SST, along with related meridional heat and moisture transports, could have played a role in the Holocene climate of the study region.

Acknowledgments

Radiocarbon ages were measured in the Key Lab. of Western China's Environmental Systems (Ministry of Education of China), Lanzhou University. Pollen analysis was conducted in the Institution of Hydrology and Environmental Geology, CAGS. We feel grateful to Prof. Cao Jixiu of Lanzhou University and Prof. Tong Guobang of the Institution of Hydrology and Environmental Geology for their help in laboratory analyses. We thank Prof. Dr. Ingmar Unkel of Kiel University for his valuable suggestions and language improvement. We sincerely thank the anonymous reviewers Senior Editor A. Gillespie, and especially Associate Editor P. J. Bartlein, for their constructive comments and suggestions. This work was supported by the Natural Science Foundation of China (Nos. 41071137 and 40671189), the Research Program of Institution of High Education in Guangdong Province for High-level Talents, and the Natural Science Foundation of Guangdong Province (Nos. 2014A030313435 and S2011010003413).

References

Aaby, B., 1976. Cyclic climatic variations in climate over the last 5500 years reflected in raised bog. Nature 263, 281–284.
An, Z.S., 2000. The history and variability of the East Asian palaeomonsoon climate. Quaternary Science Reviews 19, 171–187.
Bengtsson, L., Enell, M., 1986. Chemical analysis. In: Berglund, B.E. (Ed.), Handbook of Holocene palaeoecology and palaeo-hydrology. John Wiley & Sons Ldt, Chichester, pp. 423–451.
Berger, A., Loutre, M.F., 1991. Insolation values for the climate of the last 10 million years. Quaternary Science Reviews 10, 297–317.
Bolch, C.J.S., 1997. The use of sodium polytungstate for the separation and concentration of living dinoflagellate cysts from marine sediments. Phycologia 36, 472–478.
Bond, G., Kromer, B., Beer, J., Muscheler, R., Evans, M., Showers, W., Hoffmann, S., Lotti-Bond, R., Hajdas, I., Bonani, G., 2001. Persistent solar influence on North Atlantic climate during the Holocene. Science 294, 2130–2136.
Cai, Y.J., Tan, L.C., Cheng, H., An, Z.S., Edwards, R.L., Kelly, M.J., Kong, X.G., Wang, X.F., 2010. The variation of summer monsoon precipitation in central China since the last deglaciation. Earth and Planetary Science Letters 291, 21–31.
Chai, X., 1993. Peatland. Geological Publishing House, Beijing, pp. 139–140.
Chambers, F.M., Barber, K.E., Maddy, D., Brew, J., 1997. A 5500-year proxy-climate and vegetation record from blanket mire at Talla Moss, Borders, Scotland. The Holocene 391–399.
Charman, D.J., Caseldine, C., Barker, A., Gearey, B., Hatton, J., Proctor, C., 2001. Paleohydrological records from peat profiles and speleothems in Sutherland, North-west Scotland. Quaternary Research 55, 223–234.
Christopher, J.E., John, H., 2000. Climatic control of blanket mire development at Kentra Moss, North-west Scotland. Journal of Ecology 88, 869–889.
Dong, J.G., Wang, Y.J., Cheng, H., et al., 2010. A high-resolution stalagmite record of the Holocene East Asian monsoon from Mt Shennongjia, central China. The Holocene 20, 257–264.
Dykoski, C.A., Edwards, R.L., Cheng, H., Yuan, D.X., Cai, Y.J., Lin, Y.S., 2005. A high-resolution, absolute-dated Holocene and deglacial Asian monsoon record from Dongge Cave, China. Earth and Planetary Science Letters 233, 71–86.
Fægri, K., Iversen, J., 1989a. Textbook of Pollen Analysis. 4th edition. John Wiley and Sons, London.
Faegri, K., Iversen, J., 1989b. Textbook of Pollen Anal ysis. Wiley, New York.

https://doi.org/10.1016/j.yqres.2015.06.002 Published online by Cambridge University Press

Fleitmann, D., Burns, S.J., Mudelsee, M., Neff, U., Kramers, J., Mangini, A., Matter, A., 2003. Holocene forcing of the Indian monsoon recorded in a stalagmite from southern Oman. Science 300, 1737–1739.
Fleitmann, D., Burns, S.J., Mangini, A., Mu, D.M., Kramers, J., Villa, I., Neff, U., Al-Subbary, A.A., Buettner, A., Hippler, D., Matter, A., 2007. Holocene ITCZ and Indian monsoon dynamics recorded in stalagmites from Oman and Yemen (Socotra). Quaternary Science Reviews 26, 170–188.
Fleitmann, D., Mudelsee, M., Burns, S.J., Bradley, R.S., Kramers, J., Matter, A., 2008. Evidence for a widespread climatic anomaly at around 9.2 ka before present. Paleooceanography 23. http://dx.doi.org/10.1029/2007PA001519 (PA1102).
Gagan, M.K., Hendy, E.J., Haberle, S.G., Hantoro, W.S., 2004. Post-glacial evolution of the Indo-Pacific warm pool and El Nino–Southern Oscillation. Quaternary International 118–119, 127–143.
Gao, Y., Xu, S., Guo, Q., Zhang, M., 1962. Monsoon region and regional climate in China. In: Gao, Y., Xu, S. (Eds.), Some Problems of East Asian Monsoon. Science Press, Beijing, pp. 49–63.
Gupta, A.K., Das, M., Anderson, D.M., 2005. Solar influence on the Indian summer monsoon during the Holocene. Geophysical Research Letters 32, L17703. http://dx.doi.org/10.1029/2005GL022685.
Haug, G.H., Hughen, K.A., Sigman, D.M., Peterson, L.C., Röhl, U., 2001. Southward migration of the Intertropical Convergence Zone through the Holocene. Science 293, 1304–1308.
Heinrich, H., 1988. Origin and consequences of cyclic ice rafting in the northeast Atlantic Ocean during the past 130000 years. Quaternary Research 29, 142–152.
Heiri, O., Lotter, A.F., Lemcke, G., 2001. Loss on ignition as a method for estimating organic and carbonate content in sediments: reproducibility and comparability of results. Journal of Paleolimnology 25, 101–110.
Herzschuh, U., 2006. Palaeo–moisture evolution in monsoonal Central Asia during the last 50,000 years. Quaternary Science Reviews 25, 163–178.
Hong, Y.T., Hong, B., Lin, Q.H., Zhu, Y.X., Shibata, Y., Hirota, M., Uchida, M., Leng, X.T., Jiang, H.B., Xu, H., Wang, H., Yi, L., 2003. Correlation between Indian Ocean summer monsoon and North Atlantic climate during the Holocene. Earth and Planetary Science Letters 211, 371–380.
Hong, Y.T., Hong, B., Lin, Q.H., Shibata, Y., Hirota, M., Zhu, Y.X., Leng, X.T., Wang, Y., Wang, H., Yi, L., 2005. Inverse phase oscillations between the East Asian and Indian Ocean summer monsoons during the last 12000 years and paleo-El Niño. Earth and Planetary Science Letters 231, 337–346.
Hong, B., Hong, Y.T., Lin, Q.H., Shibata, Y., Uchida, M., Zhu, Y.X., Leng, X.T., Wang, Y., Cai, C.C., 2010. Anti-phase oscillation of Asian monsoons during the Younger Dryas period: evidence from peat cellulose $\delta^{13}C$ of Hani, Northeast China. Palaeogeography Palaeoclimatology Palaeoecology 297, 214–222.
Hu, C., Henderson, G.M., Huang, J., Xie, S., Sun, Y., Johnson, K.R., 2008. Quantification of Holocene Asian monsoon rainfall from spatially separated cave records. Earth and Planetary Science Letters 266, 221–232.
Huang, R., Huang, G., Wei, Z.G., 2004. Climate variations of the summer monsoon over China. In: Chang, C.P. (Ed.), East Asian Monsoon. World Scientific Publishing Co. Pte. Ltd, Singapore, pp. 213–268.
Ivanochko, T.S., Ganeshram, R.S., Brummer, G.J.A., Ganssen, G., Jung, S.J.A., Moreton, S.G., Kroon, D., 2005. Variations in tropical convection as an amplifier of global climate change at the millennial scale. Earth and Planetary Science Letters 235, 302–314.
Janssens, J.A., 1983. A quantitative method for stratigraphic analysis of bryophytes in Holocene peat. Journal of Ecology 171, 189–196.
Ji, J.F., Shen, J., Balsam, W., Chen, J., Liu, L.W., Liu, X.Q., 2005. Asian monsoon oscillations in the northeastern Qinghai–Tibet Plateau since the late glacial as interpreted from visible reflectance of Qinghai Lake sediments. Earth and Planetary Science Letters 233, 61–70.
Jian, Z., Wang, P., Saito, Y., Wang, J., Pflauman, U., Oba, T., Cheng, X., 2000. Holocene variabil-ity of the Kuroshio Current in the Okinawa Trough, northwestern Pacific Ocean. Earth and Planetary Science Letters 184, 305–319.
Jiang, X.Y., He, Y.Q., Shen, C.C., Kong, X.G., Li, Z.Z., Chang, Y.W., 2012. Stalagmite-inferred Holocene precipitation in northern Guizhou Province, China, and asynchronous termination of the Climatic Optimum in the Asian monsoon territory. Chinese Science Bulletin 57, 795–801.
Kienast, M., Steinke, S., Stattegger, K., Calvert, S.E., 2001. Synchronous tropical South China Sea sea surface temperature change and Greenland warming during deglaciation. Science 291, 2132–2134.
Lea, D.W., Pak, D.K., Spero, H.J., 2000. Climate impact of late Quaternary Equatorial Pacific sea surface temperature variations. Science 289, 1719–1724.
Liew, P.M., Lee, C.Y., Kuo, C.M., 2006. Holocene thermal optimal and climate variability of East Asian monsoon inferred from forest reconstruction of a subalpine pollen sequence, Taiwan. Earth and Planetary Science Letters 250, 596–605.
Liu, M.S., Hong, B.G., 1998. The distribution of Fagaceas in China and its relationship with climatic and geographic characters. Acta Phytoecologica Sinica 22, 41–50.
Liu, Z., Brady, E., Lynch-Stieglitz, J., 2003. Global ocean response to orbital forcing in the Holocene. Paleoceanography 18 (2), 1041.
Liu, J., Wang, B., Yang, J., 2008. Forced and internal modes of variability of the East Asian summer monsoon. Climate of the Past 2, 225–233.
Overpeck, J., Anderson, D., Trumbore, S., Prell, W., 1996. The southwest Indian Monsoon over the last 18000 years. Climate Dynamics 12, 213–225.
Qian, W., Lin, X., Zhu, Y., Xu, Y., Fu, J., 2007. Climatic regime shift and decadal anomalous events in China. Climatic Change 84, 167–189.
Reimer, P.J., Baillie, M.G.L., Bard, E., et al., 2009. IntCal09 and Marine09 radiocarbon age calibration curves, 0–50,000 years cal BP. Radiocarbon 51, 1111–1150.
Selvaraj, K., Chen, C.T.A., Lou, J.Y., 2007. Holocene East Asian monsoon variability: links to solar and tropical Pacific forcing. Geophysical Research Letters 34, L01703.
Shi, Y.F., Kong, Z.C., Wang, S.M., Tang, L.Y., Wang, F.B., Yao, T.D., Zhao, X.T., Zhang, P.Y., Shi, S.H., 1993. The climate and environment during the Holocene megathermal maximum in China. Science in China (Series B) 23, 865–873 (in Chinese).
Shinozaki, T., Uchida, M., Minoura, K., Kondo, M., Rella, S.F., Shibata, Y., 2011. Synchronicity of the East Asian Summer Monsoon variability and Northern Hemisphere climate change since the last deglaciation. Climate of the Past Discussions 7, 2159–2192.
Stanford, J.D., Rolling, E.J., Bacon, S., Roberts, A.P., Grousset, F.E., Bolshaw, M., 2011. A new concept for the paleoceanographic evolution of Heinrich event 1 in the North Atlantic. Quaternary Science Reviews 30, 1047–1066.
Stebich, M., Mingram, J., Moschen, R., Thiele, A., Schröder, C., 2011. Comments on"Anti-phase oscillation of Asian monsoons during the Younger Dryas period: evidence from peat cellulose $\delta^{13}C$ of Hani, Northeast China" by B Hong, YTHong, QH Lin, Yasuyuki Shibata, Masao Uchida, YX Zhu, XT Leng, Y Wang and CC Cai [Palaeogeography, Palaeoclimatology, Palaeoecology 297 (2010): 214-222]. Palaeogeography Palaeoclimatology Palaeoecology 310, 464–470.
Stott, L., Cannariato, K., Thunell, R., 2004. Decline of surface tempera-ture and salinity in the western tropical Pacific Ocean in the Holocene epoch. Nature 431, 56–59.
Sun, S.Y., Zhang, J.E., 1984. Pollen combination of the Daping peat deposit in Hunan and its formation environment. Journal Nanjing Normal University 4, 86–92 (in Chinese).
Wang, L., Sarnthein, M., Erlenkeuser, H., Grimalt, J., Grootes, P., Heilig, S., Ivanova, E., Kienast, M., Pelejero, C., Pflaumann, U., 1999. East Asian monsoon climate during the Late Pleistocene: high-resolution sediment records from the South China Sea. Marine Geology 156, 245–284.
Wang, Y.J., Cheng, H., Edwards, R.L., An, Z.S., Wu, J.Y., Shen, C.C., Dorale, J.A., 2001. A high–resolution absolute–dated late Pleistocene monsoon record from Hulu Cave, China. Science 294, 2345–2348.
Wang, Y.J., Cheng, H., Edwards, R.L., He, Y., Kong, X., An, Z.S., Wu, J., Kelly, M.J., Dykoski, C.A., Li, X., 2005. The Holocene Asian monsoon: links to solar changes and North Atlantic climate. Science 308, 854–857.
Wang, S.Y., Lü, H.Y., Liu, J.Q., Negendank, J.F.W., 2007. The early Holocene optimum inferred from a high–resolution pollen record of Huguangyan Maar Lake in southern China. Chinese Science Bulletin 52, 2829–2836.
Wang, X.F., Cruz, F.W., Auler, A.S., Cheng, H., Edward, R.L., 2008a. Millennial–scale climate variability recorded in Brazilian speleothems. PAGES News 16, 31–32.
Wang, Y.J., Cheng, H., Edwards, R.L., Kong, X., Shao, X., Chen, S., Wu, J., Jiang, X., Wang, X., An, Z., 2008b. Millennial- and orbital-scale changes in the East Asian monsoon over the past 224,000 years. Nature 451, 1090–1093.
Wang, H., Hong, Y.T., Lin, Q.H., Hong, B., Zhu, Y.X., Wang, Y., Xu, H., 2010. Response of humification degree to monsoon climate during the Holocene from the Hongyuan peat bog, eastern Tibetan Plateau. Palaeogeography Palaeoclimatology Palaeoecology 286, 171–177.
Wu, W., Liu, T., 2005. Possible role of the "Holocene Event 3" on the collapse of Neolithic Cultures around the Central Plain of China. Quaternary International 117, 153–166.
Xiao, Y.T., Cao, T.R., Pen, Z.H., 1986. Mapping the vegetation (1:50000) of the Nanshan Mountain of Chengbu county, Huanan Province. Journal of Central-South Forestry College 6, 34–40 (in Chinese).
Xiao, J.Y., Lu, H.B., Zhou, W.J., Zhao, Z.J., Hao, R.H., 2007. Evolution of vegetation and climate since the last glacial maximum recorded at Dahu peat site, South China. Science in China Series D: Earth Sciences 50, 1209–1217.
Yancheva, G., Nowaczyk, N.R., Mingram, J., Dulski, P., Schettler, G., Negendank, J.F.W., Liu, J.Q., Sigman, D.M., Peterson, L.C., Haug, G.H., 2007. Influence of the intertropical convergence zone on the East Asian monsoon. Nature 445, 74–77.
Yao, T.D., Jiao, K.Q., Tian, L.D., Yang, Z., Shi, W., 1996. Climatic variations since the Little Ice Age recorded in Guliya Ice Core. Science in China (Series D) 39, 587–596.
Zabenskie, S., Peros, M., Gajewski, K., 2006. The use of heavy-liquid in the separation of pollen from Arctic lake sediments. Canadian Association Palynology Newsletter 29, 5–7.
Zhang, J.W., Chen, F.H., Holmes, J.A., Li, H., Guo, X.Y., Wang, J.L., Li, S., Lü, Y.B., Zha, Y., Qiang, M.R., 2011. Holocene monsoon climate documented by oxygen and carbon isotopes from lake sediments and peat bogs in China: a review and synthesis. Quaternary Science Reviews 30, 1973–1987.
Zhang, H.L., Yu, K.F., Zhao, J.X., Feng, Y.X., Lin, Y.S., Zhou, W., Liu, G.H., 2013. East Asian Summer Monsoon variations in the past 12.5 ka: high-resolution $\delta^{18}O$ record from a precisely dated aragonite stalagmite in Central China. Journal of Asian Earth Sciences http://dx.doi.org/10.1016/j.jseaes.2013.04.015.
Zhong, W., Xue, J.B., Zheng, Y.M., Ouyang, J., Ma, Q.H., Cai, Y., Tang, X.H., 2010a. Climatic changes since the last deglaciation inferred from a lacustrine sedimentary sequence in the eastern Nanling Mountains, south China. Journal of Quaternary Science 25, 975–984.
Zhong, W., Ma, Q.H., Xue, J.B., Zheng, Y.M., Cai, Y., Ouyang, J., 2010b. Humification degrees of a lacustrine sedimentary sequence as an indicator of past climatic changes in the last c. 49 000 years in South China. Boreas 39, 286–295.
Zhong, W., Xue, J.B., Ouyang, J., Cao, J.Y., Peng, Z.H., 2014. Evidence of late Holocene climate variability in the western Nanling Mountains, South China. Journal of Paleolimnology 52, 1–10.
Zhou, W.J., Yu, X.F., Timothy, J.A.J., Burr, G., Xiao, J.Y., Lu, X.F., Xian, F., 2004. High–resolution evidence from southern China of an early Holocene optimum and a mid–Holocene dry event during the past 18,000 years. Quaternary Research 62, 39–48.
Zhou, H.Y., Feng, Y.X., Zhao, J.X., Shen, C.C., You, C.F., Lin, Y., 2009. Deglacial variations of Sr and $^{87}Sr/^{86}Sr$ ratio recorded by a stalagmite from Central China and their association with past climate and environment. Chemical Geology 268, 233–247.

https://doi.org/10.1016/j.yqres.2015.06.002 Published online by Cambridge University Press